



Characteristics of Elovich equation used for the analysis of adsorption kinetics in dye-chitosan systems

Feng-Chin Wu^a, Ru-Ling Tseng^{b,*}, Ruey-Shin Juang^{c,d}

^a Department of Chemical Engineering, National United University, Miao-Li 360, Taiwan

^b Department of Safety, Health and Environmental Engineering, National United University, No. 1, Lien Da, Kung-Ching Li, Miao-Li 360, Taiwan

^c Department of Chemical Engineering and Materials Science, Yuan Ze University, Chung-Li 32003, Taiwan

^d Fuel Cell Center, Yuan Ze University, Chung-Li 32003, Taiwan

ARTICLE INFO

Article history:

Received 14 October 2008

Received in revised form 3 January 2009

Accepted 8 January 2009

Keywords:

Adsorption

Chitosan

Kinetic models

Elovich equation

ABSTRACT

The Elovich equation has been widely used in adsorption kinetics, which describes chemical adsorption (chemical reaction) mechanism in nature. The approaching equilibrium parameter of Elovich equation (R_E) was used here to describe the characteristic curves of adsorption kinetics. Of 64 adsorption systems surveyed in this work, 80% of the R_E values were between 0.1 and 0.3 with an adsorption curve belonging to “mild rising”. The results of three examples revealed that the characteristic curve of Elovich equation was between those of Lagergren’s first-order equation and intraparticle diffusion model. Chitosans prepared from prawn, lobster, and crab shells were used for the adsorption of a reactive dye. The mean deviation obtained from the three kinetic models revealed that Elovich equation was the most suitable one. All the adsorption systems were in the “mild rising” zone. The R_E value was related to the type of raw material but not to the particle size of chitosan, which agreed with chemical adsorption nature of the Elovich equation. According to an optimal adsorbent consumption of 85% coupled with its corresponding operating time ($t_{0.85}$) proposed, these two parameters could be used for engineering design.

© 2009 Published by Elsevier B.V.

1. Introduction

The Elovich equation, originally presented in 1939, is satisfied in chemical adsorption processes and is suitable for systems with heterogeneous adsorbing surfaces [1]. In the past, this equation has been applied in the adsorption of Co^{2+} , Ni^{2+} , Cu^{2+} , and Zn^{2+} on XAD-2 resin containing di(2-ethylhexyl)phosphoric acid [2], of dyes and humic acid on chitosan-encapsulated activated carbon [3], and of dyes and phenols on activated carbon [4]. Many adsorption systems with metals (Pb^{2+} , Cr^{3+} , Cr^{6+} , Cd^{2+} , Cu^{2+} , Se^{4+} , As^{5+} , K^+ , Pb^{2+} , etc.) have been described by Elovich equation [5–13]. The kinetic behavior of many adsorption systems with a mildly rising tendency has also suitably been described by Elovich equation (no shown).

Chitosan is a biopolymer with free amine groups that suitable for the adsorption of metals and reactive dyes. The adsorption process involving chitosan is chemical in nature and its kinetic behavior is mildly rising [14–16]; however, the Elovich equation has scarcely been used to analyze its adsorption kinetics. In this work, the characteristic curves of adsorption kinetics by Elovich equation were studied by means of its approaching equilibrium parameter (R_E).

Several adsorption systems selected from literature were analyzed by Elovich equation to determine the distribution of R_E values. Chitosans prepared from three kinds of raw materials (prawn shell, lobster shell, and crab shell) as well as the lobster-shell chitosans with three different particle sizes were used to investigate the kinetics of the adsorption of dye (reactive red 222, RR222). Three kinetic models (Elovich equation, Lagergren’s first-order equation, and intraparticle diffusion model) were tried to analyze the kinetic data. The effects of material source and particle size of chitosan adsorbents on R_E value were finally examined.

2. Kinetic models

2.1. Characteristic curve and approaching equilibrium of the Elovich equation

In reactions involving chemical adsorption of gases on a solid surface without desorption of the products, the rate decreases with time due to an increase in surface coverage [1]. One of the most useful models for describing such activated chemical adsorption is the Elovich equation [2], which is given by

$$\left(\frac{dq_t}{dt}\right) = a \exp(-bq_t) \quad (1)$$

* Corresponding author. Tel.: +886 37 381775; fax: +886 37 333187.
E-mail address: trl@nuu.edu.tw (R.-L. Tseng).

Nomenclature

a	initial adsorption rate defined in Eq. (1) (mg/(g min))
AC	activated carbon
BDTDA	benzyltrimethyl tetradecyl ammonium chloride
b	Elovich constant defined in Eq. (1) (g/mg)
CV	crystal violet
C	constant defined in Eq. (8) (mg/g)
CP	chlorophenol
DCP	dichlorophenol
FTAW	formaldehyde treated acorn waste
HDTMA	hexadecyl trimethyl ammonium bromide
ID	intraparticle diffusion
k_1	Lagergren's first-order rate constant defined in Eq. (11) (min^{-1})
k_p	ID rate constant defined in Eq. (8) ($\text{mg}/(\text{g min}^{1/2})$)
LAS	linear alkyl sulfonate
MB	methylene blue
MG	methylene green
MOCS	manganese oxide coated sand
NP	nitrophenol
q_e	amount of adsorption at equilibrium (mg/g)
q_{ref}	amount of adsorption at time $t = t_{ref}$ (mg/g)
q_t	amount of adsorption at time $t = t$ (mg/g)
r^2	coefficient of correlation
R_E	approaching equilibrium parameter based on Elovich equation
R_i	starting adsorption factor based on ID model
SD	standard deviation defined in Eq. (16) (%)
t	adsorption time (min)
t_{ref}	the longest operating time in adsorption process (min)
x	fractional approach to q_{ref}

where a and b are constants during any an experiment. The constant a is regarded as the initial rate because (dq_t/dt) approaches a when q_t approaches 0.

Given that $q_t = q_t$ at $t = t$ and $q_t = 0$ at $t = 0$, the integrated form of Eq. (1) is

$$q_t = \left(\frac{1}{b}\right) \ln(t + t_0) - \left(\frac{1}{b}\right) \ln t_0 \quad (2)$$

where $t_0 = 1/ab$. If $t \gg t_0$, Eq. (2) can be simplified as

$$q_t = \left(\frac{1}{b}\right) \ln(ab) + \left(\frac{1}{b}\right) \ln t \quad (3)$$

The assumption of $t \gg t_0$ and validity of Eq. (3) is checked by the linear plot of q_t vs. $\ln t$.

For an adsorption system, let t_{ref} be the longest time in adsorption process and q_{ref} the solid phase concentration at time $t = t_{ref}$. Thus, Eq. (3) is rewritten as

$$q_{ref} = \left(\frac{1}{b}\right) \ln(ab) + \left(\frac{1}{b}\right) \ln t_{ref} \quad (4)$$

Subtracting Eq. (4) from Eq. (3), we have:

$$q_t - q_{ref} = \left(\frac{1}{b}\right) \ln \left(\frac{t}{t_{ref}}\right) \quad (5)$$

Dividing both sides of Eq. (5) by q_{ref} yields:

$$\left(\frac{q_t}{q_{ref}}\right) = \left(\frac{1}{q_{ref}b}\right) \ln \left(\frac{t}{t_{ref}}\right) + 1 \quad (6)$$

Eq. (6) is called dimensionless Elovich equation. Define $R_E = 1/(q_{ref}b)$ as approaching equilibrium factor of the Elovich equation; thus Eq.

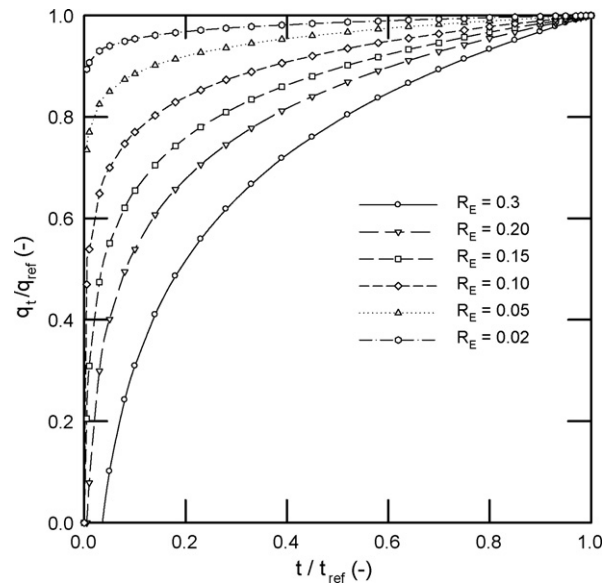


Fig. 1. Characteristic curves based on dimensionless Elovich equation (R_E is the approaching equilibrium parameter of Elovich equation).

(6) is rewritten as

$$\left(\frac{q_t}{q_{ref}}\right) = R_E \ln \left(\frac{t}{t_{ref}}\right) + 1 \quad (7)$$

A family of adsorption characteristics are obtained by plotting (q_t/q_{ref}) vs. (t/t_{ref}) of Eq. (7) with $R_E = 0.02$ – 0.3 and are shown in Fig. 1. The curves vary with R_E value, appearing either flat or steep. According to the curvature of the curves, which depends on R_E values, four zones are classified: when $R_E > 0.3$ (zone I), the curve rises slowly; when R_E between 0.1 and 0.3 (zone II), the curve rises mildly; when R_E is between 0.02 and 0.1 (zone III), the curve rises rapidly; when the $R_E < 0.02$ (zone IV), the curve instantly approaches equilibrium. These zones and the corresponding curves are given in Table 1.

2.2. Comparisons of characteristic curves

Besides Elovich equation, intraparticle diffusion (ID) model and the Lagergren's first-order equation were also frequently used to describe adsorption kinetics. An attempt was made to compare them in this work. Simply input, ID model has the form:

$$q_t = k_p t^{1/2} + C \quad (8)$$

At $t = t_{ref}$, $q_t = q_{ref}$, Eq. (8) is rewritten as

$$q_{ref} = k_p t_{ref}^{1/2} + C \quad (9)$$

Subtracting Eq. (9) from Eq. (8), we obtain:

$$\left(\frac{q_t}{q_{ref}}\right) = 1 - R_i \left[1 - \left(\frac{t}{t_{ref}}\right)^{1/2}\right] \quad (10)$$

where $R_i = (k_p t_{ref}^{1/2}/q_{ref})$ is the starting adsorption factor of ID model (dimensionless).

Table 1
Classification of characteristic curves based on the approaching equilibrium parameter (R_E) derived from the Elovich equation.

R_E	Curve	Zone
$R_E > 0.3$	Slow rising	I
$0.3 > R_E > 0.1$	Mild rising	II
$0.1 > R_E > 0.02$	Rapid rising	III
$R_E < 0.02$	Instant approaching equilibrium	IV

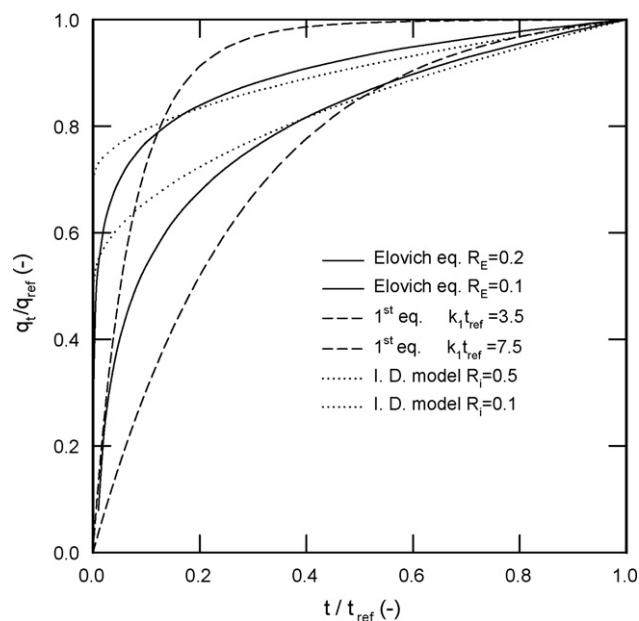


Fig. 2. Characteristic curves based on dimensionless Elovich equation, intraparticle diffusion model, and Lagergren's first-order equation (R_E is the approaching equilibrium parameter of Elovich equation, R_i is the starting adsorption parameter of intraparticle diffusion model, and $k_1 t_{ref}$ is the approaching equilibrium parameter of Lagergren's first-order equation).

On the other hand, the Lagergren's first-order equation is expressed as

$$\ln(q_e - q_t) = \ln q_e - k_1 t \quad (11)$$

Usually, k_1 is obtained by plotting $\ln(q_e - q_t)$ vs. t . For expressing adsorption characteristics of this equation, Eq. (11) is rewritten as

$$\ln \left[1 - \left(\frac{q_t}{q_e} \right) \right] = -k_1 t \quad (12)$$

When both sides of Eq. (12) are divided by t_{ref} , the longest adsorption time in the system, we get:

$$\left(\frac{q_t}{q_e} \right) = 1 - \exp \left[(-k_1 t_{ref}) \left(\frac{t}{t_{ref}} \right) \right] \quad (13)$$

For an adsorption system, let q_t be q_{ref} at time $t = t_{ref}$; thus:

$$\left(\frac{q_{ref}}{q_e} \right) = 1 - \exp(-k_1 t_{ref}) \quad (14)$$

Dividing Eq. (13) by Eq. (14) yields:

$$\left(\frac{q_t}{q_{ref}} \right) = 1 - \frac{\exp[(-k_1 t_{ref})(t/t_{ref})]}{[1 - \exp(-k_1 t_{ref})]} \quad (15)$$

Eqs. (10) and (15) are the dimensionless characteristic kinetic equations based on ID model and the Lagergren's first-order equation, respectively. If (q_t/q_{ref}) vs. (t/t_{ref}) is plotted with R_i or $k_1 t_{ref}$ as a parameter, both families of characteristic curves can be obtained.

When the above three kinetic model are used to describe the data set adsorption system, three kind of curves appear close to the data set. Fig. 2 shows the characteristic curves based on the Elovich equation (Eq. (7)) with $R_E = 0.1$ and 0.2 , based on ID model (Eq. (10)) with $R_i = 0.1$ and 0.5 , and based on Lagergren's first-order equation (Eq. (15)) with $k_1 t_{ref} = 3.5$ and 7.5 . The curves obtained in each model appear similar tendency. The curves of Lagergren's first-order equation have a high adsorption over a longer time and flat-rising with a shorter duration, whereas those of ID model have a high adsorption for a shorter period of time and flat-rising with a longer duration. The curves of Elovich equation are between those of the above two models. In most of the literature, adsorption based

on Elovich equation rise rapidly with a shorter time rises slightly with a longer time (no shown).

3. Materials and methods

3.1. Preparation of chitosan from fishery waste

In this work, chitosan was prepared from three fishery wastes (prawn, lobster, and crab shells). The shells were first immersed in 5 wt.% NaOH for 18 h to remove proteins (solid shells/solution = 10%, w/v) and in 10 wt.% HCl for 18 h to remove all mineral materials (mainly, CaCO_3). The resulting insoluble solid is chitin, which (40 g) was then deacetylated in 50 wt.% NaOH (800 g) at 90°C for 3 h. The final chitosan particles were filtered and washed several times with deionized water. They were dried at 50°C in a vacuum for 12 h and then sieved with a 16–30 mesh. In this work, chitosans prepared from prawn, lobster, and crab shells, and were called chitosan 1, chitosan 2, and chitosan 3, respectively. Moreover, chitosan prepared from lobster shells was crashed and sieved within 20–30, 30–40, and 40–50 mesh, which were called DP1, DP2, and DP3, respectively.

The degree of deacetylation of chitosan was measured according to the method used by Guibal et al. [17]. The molar mass of chitosan was determined using the Mark–Houwink equation for viscosity measurements at different concentrations.

3.2. Procedures for adsorption experiments

The commercial reactive dye Sumifix Super Scarlet 2GF (reactive red 222, RR222) from Summitomo Chemical Co., Japan was used as received. It has vinyl sulfone/monochlorotriazine bifunctional groups. The solutions were prepared by dissolving dye in deionized water without pH adjustment, in which the initial pH value was near 5.32.

The batch contact was conducted in a Pyrex glass vessel of 100 mm i.d. and 130 mm high, fitted with four glass baffles, 10 mm wide. For each run, an aqueous solution (0.8 dm^3) agitated by using a Cole–Parmer Servodyne agitator with six blade, flat-bladed impeller (12 mm high, 40 mm wide). The stirring speed was 500 rpm because higher than that the agitation has little effect on adsorption. An amount of dry chitosan (0.48 g) was then added to the vessel and the timing was started. The whole vessel was immersed in a water bath controlled at 30°C (Haake Model K-F3). At preset time intervals, aqueous samples (5 cm^3) were taken and the concentration was analyzed. The concentration of dye was determined with a Hitachi UV/visible spectrophotometer (U-2001) at a wavelength of 502 nm. Each experiment was duplicated at least under identical conditions.

4. Results and discussion

4.1. Physical properties of chitosans

As shown in Table 2, the degree of deacetylation of chitosan prepared from prawn shells is the highest (80.9%), and that from lobster shells is the lowest (76.3%). The molar mass of the three chitosans prepared is comparable, between 7.44×10^5 and $7.93 \times 10^5 \text{ g/mol}$.

Table 2
Degree of deacetylation and molecular weight of various chitosans.

Adsorbent	Raw material	Degree of deacetylation (%)	Chitin (g) ^a	Chitosan (g) ^a	Molar mass (g/mol)
Chitosan 1	Prawn shell	80.9	21.0	14.6	7.93×10^5
Chitosan 2	Lobster shell	76.3	10.8	8.3	7.97×10^5
Chitosan 3	Crab shell	77.9	17.3	12.7	7.44×10^5

^a Basis: 100 g of fishery wastes.

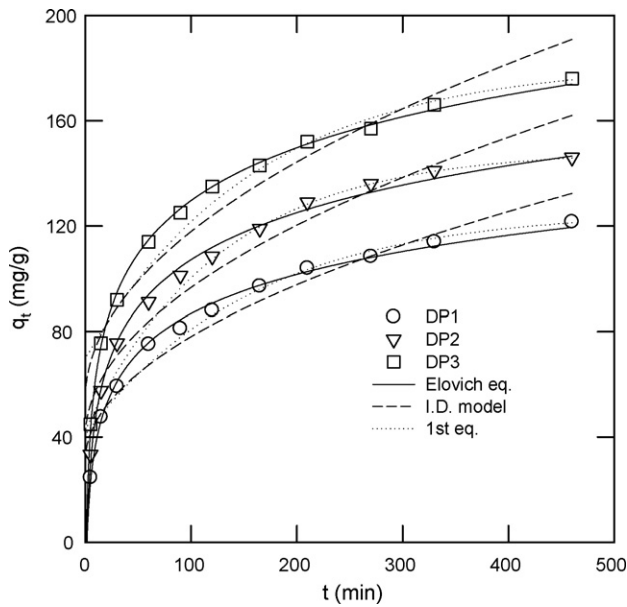


Fig. 3. Regression analysis of the adsorption of RR222 on chitosans with different particle sizes by Elovich equation, intraparticle diffusion model, and Lagergren's first-order equation.

4.2. Adsorption kinetics and validity of kinetic models

Fig. 3 shows the experimental data in the adsorption of RR222 on chitosans with three different particle sizes (that is, DP1, DP2, and DP3), together with the curves calculated from the three kinetic models. It is found that Elovich equation is superior to other two ones for the description of kinetic data. The fitness is justified based on the fact that the coefficients of correlation (r^2) are within 0.995–0.998, 0.982–0.996, and 0.925–0.935, respectively (Tables 3 and 4). Moreover, the standard deviation (S.D.) is provided in these two tables to infer the validity of kinetic models, defined as

$$\text{S.D.}(\%) = 100 \times \left\{ \frac{\sum_N (1 - (q_{t,\text{cal}}/q_{t,\text{exp}}))^2}{N} \right\}^{1/2} \quad (16)$$

Table 3

Parameters and correlation coefficients obtained from the analysis of adsorption kinetics by Elovich equation.

Adsorbent	a (mg/(g min))	b (g/mg)	t_0 (min)	q_{ref} (mg/g)	R_E	r^2	S.D. (%)
DP1	12.32	0.0467	1.74	119	0.180	0.996	3.5
DP2	16.43	0.0388	1.57	147	0.175	0.995	4.2
DP3	25.38	0.0345	1.14	174	0.167	0.998	2.0
Chitosan 1	54.96	0.0193	1.06	299	0.173	0.998	1.4
Chitosan 2	14.95	0.0342	0.51	147	0.199	0.997	3.5
Chitosan 3	9.384	0.0453	0.43	107	0.206	0.981	7.2

Table 4

Parameters and correlation coefficients obtained from the analysis of adsorption kinetics by the Lagergren's first-order equation and intraparticle diffusion model.

Adsorbent	Lagergren's first-order equation				Intraparticle diffusion model			
	q_e (mg/g)	k_1 (min ⁻¹)	r^2	S.D. (%)	q_i (mg/g)	k_i^a	r^2	S.D. (%)
DP1	126	0.00636	0.987	14.4	30.6	4.74	0.935	14.2
DP2	149	0.00785	0.996	11.6	39.6	5.71	0.931	13.3
DP3	182	0.00620	0.982	13.1	54.1	6.38	0.925	12.6
Chitosan 1	319	0.00819	0.979	12.5	93.9	13.2	0.932	11.8
Chitosan 2	158	0.00866	0.986	14.4	31.0	7.50	0.945	14.0
Chitosan 3	127	0.00645	0.981	16.3	18.3	5.76	0.967	14.2

^a Unit of k_i : (mg/(g min^{1/2})).

where $q_{t,\text{exp}}$ and $q_{t,\text{cal}}$ are the experimental and calculated q_t values, respectively, and N is the number of data points.

Fig. 4 shows the regression results for the adsorption of RR222 on three different types of chitosans by Elovich equation, Lagergren's first-order equation, and ID model, respectively. The coefficients of correlation are within 0.981–0.998, 0.979–0.986 and 0.932–0.967, and the S.D. values are within 1.4–7.2%, 11.6–16.3%, and 11.8–14.2%, respectively. This also reveals that Elovich equation is the most suitable for this purpose than other two models, as have confirmed in Fig. 5.

4.3. Classification of characteristic curves based on Elovich equation

Table 5 lists the analysis results of 64 adsorption systems by Elovich equation from literature, together with the longest adsorption time (t_{ref}), adsorption amount at time t_{ref} (q_{ref}), and the approaching equilibrium factor (R_E). Basically, the coefficient of correlation (r^2) for linear fit of the kinetic data reported in Table 5 by Elovich equation (Eq. (3)) is larger than 0.95. Evidently, there are no systems in the region $R_E < 0.02$ (zone IV, with an adsorption curve in “instant approaching equilibrium”) and in the region $R_E > 0.3$ (zone I, with an adsorption curve in “slowly rising”). On the other hand, there are 13 systems (No. 1–13, 20.3%) in the region $0.1 > R_E > 0.02$ (zone III, with an adsorption curve in “rapidly rising”) and 51 systems (No. 14–64, 79.7%) in the region $0.3 > R_E > 0.1$ (zone II, with an adsorption curve in “mildly rising”).

Of the adsorption systems surveyed in Table 5, the lack of zones I and IV actually agrees with the nature of chemical adsorption in Elovich equation. The main distribution of zone II makes Elovich equation suitable for the majority of adsorption systems. For example, the R_E values of the adsorption of RR222 on chitosans demonstrate that they all fall in zone II with “mildly rising” adsorption curves.

4.4. Application of Elovich equation in adsorption kinetics

As indicated above, the Elovich equation is suitable to describe adsorption behavior that concurs with the nature of chemical adsorption [1,2]. The R_E values of chitosans with three different particle sizes close each other. The plot of (q_t/q_{ref}) vs. (t/t_{ref}) (Fig. 6a) shows that the curves of chitosans with three particle sizes are almost the same. On the other hand, the adsorption of RR222 on

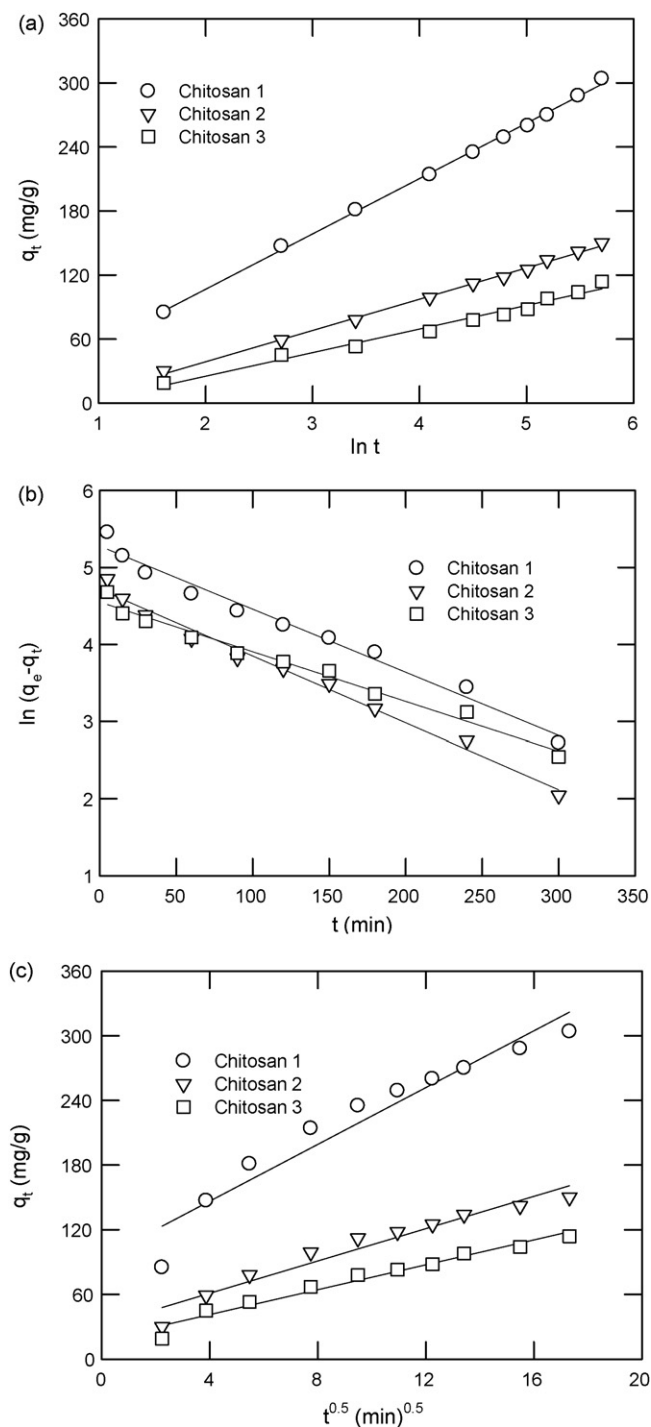


Fig. 4. Regression analysis of the adsorption of RR222 on chitosans prepared from three raw materials by (a) Elovich equation, (b) Lagergren's first-order equation, and (c) intraparticle diffusion model.

chitosans from different raw materials, as shown in Fig. 6b, shows that the adsorption on lobster- and crab-shell chitosans are similar, which are slower than that on prawn-shell chitosan. This is likely because of some differences in the chemical properties of chitosans from different origins (e.g., the degree of deacetylation of prawn-shell chitosan is the highest).

For the adsorption systems described suitably by the Elovich equation, it is important to determine an efficient operating time of adsorption in engineering practice. Let $(q_t/q_{ref}) = x$ at $t = t_x$. Then,

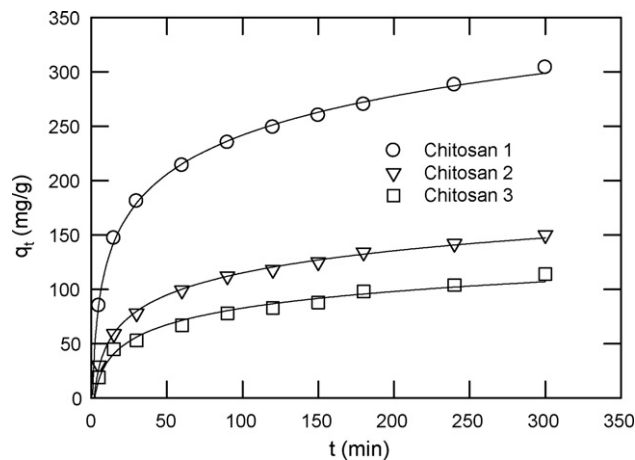


Fig. 5. Predictions of the Elovich equation in the adsorption of RR222 on chitosans prepared from different raw materials.

Eq. (7) becomes:

$$x = R_E \ln \left(\frac{t_x}{t_{ref}} \right) + 1 \quad (17)$$

or

$$\left(\frac{t_x}{t_{ref}} \right) = \exp \left[\frac{(x-1)}{R_E} \right] \quad (18)$$

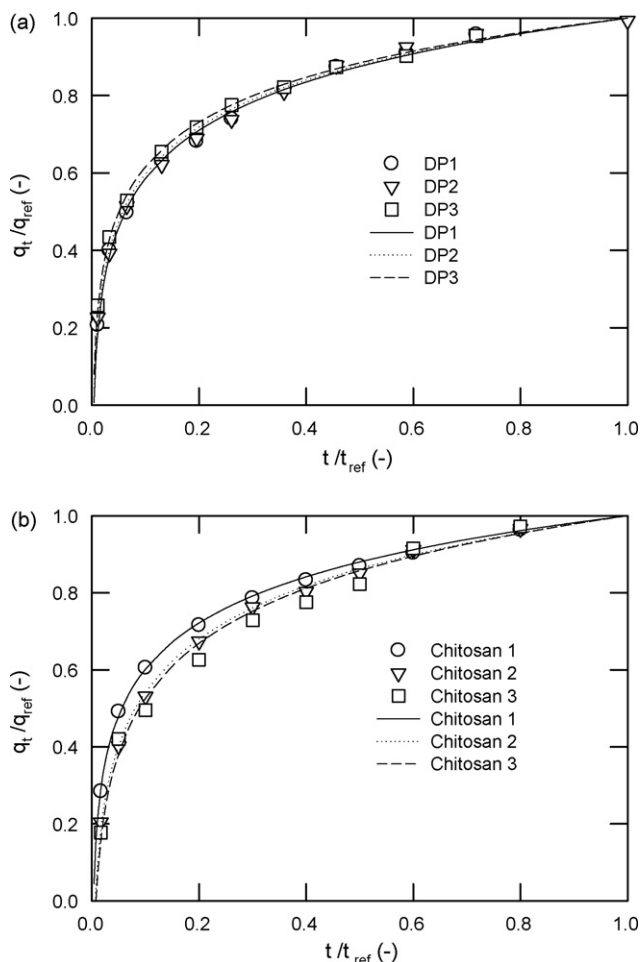


Fig. 6. Dimensionless characteristic curves of the adsorption of RR222 on (a) chitosans with three particle sizes and (b) chitosans from three raw materials.

Table 5
Survey of kinetic results of previous adsorption systems analyzed by the Elovich equation.

No.	Adsorbate	Adsorbent	a (mg/(g min))	b (g/mg)	t_{ref} (min)	q_{ref} (mg/g)	R_E	Ref.
1	3-CP	Pinewood AC	4.4E18	0.2083	210	224	0.021	[4]
2	Phenol	HDTMA-zeolite	4.04E11	16.3	1440	2.257	0.027	[18]
3	Phenol	Pinewood AC	3.28E9	0.1754	210	145	0.039	[4]
4	Se(IV)	Tropical soil	2.01E7	0.1906	1440	118	0.044	[12]
5	AB264	Pinewood AC	3.60E8	0.0307	210	721	0.045	[4]
6	Phenol	BDTDA-zeolite	9.94E4	8.27	1440	2.53	0.048	[18]
7	Phosphate	Iron oxide tailings	2.5E4	2.44	1440	7.50	0.055	[19]
8	Se(IV)	Tropical soil	2.72E4	0.0566	1440	258	0.068	[12]
9	BB69	Pinewood AC	1.18E5	0.0278	210	484	0.074	[4]
10	As(V)	Tropical soil	4.30E3	0.0366	1440	337	0.081	[12]
11	Cr(IV)	Composite	3.23E4	0.0133	420	910	0.083	[7]
12	<i>o</i> -Cresol	Pinewood AC	7.90E3	0.0725	210	161	0.085	[4]
13	Phenol	AC (FWKC1060)	2.82E4	0.0591	30	183	0.092	[20]
14	NH ₄ ⁺	Clinoptilolite (N)	4.70E3	1.44	120	6.43	0.108	[13]
15	K ⁺	Clinoptilolite (N)	1.13E4	0.432	120	21.3	0.109	[13]
16	MB	Pinewood AC	1.76E3	0.0231	210	392	0.110	[4]
17	Phenol	AC (CobNa50)	5.95E3	0.0361	30	243	0.114	[21]
18	4-CP	AC (CPKC3)	6.90E3	0.0260	30	328	0.117	[22]
19	Pb(II)	MOCS	2.92	4.97	180	1.59	0.127	[11]
20	Cu(II)	MOCS	0.543	24.9	180	0.314	0.128	[11]
21	<i>p</i> -Cresol	AC (CPKC3)	2.22E3	0.0313	30	244	0.131	[22]
22	2,4-DCP	AC (CobNa50)	7.62E3	0.0087	30	873	0.132	[21]
23	As(III)	Tropical soil	478	0.0516	1440	147	0.132	[12]
24	Cr(II)	Cation exchanger	19.7	0.26	360	28.9	0.133	[10]
25	MG	Apricot AC	352	0.083	60	90.0	0.134	[23]
26	Cr(VI)	Waste acorn	40.9	0.240	180	31.2	0.134	[9]
27	4-CP	AC (FWKC1060)	2.25E3	0.0212	30	343	0.137	[20]
28	4-NP	AC (CPKC3)	2.28E3	0.0215	30	339	0.137	[22]
29	MB	Apricot AC	218	0.088	60	80.1	0.142	[23]
30	SiO ₂	Fe/Cr hydroxide	18.4	1.050	50	6.55	0.145	[24]
31	LAS	Chitosan bead	38.7	0.089	270	76.8	0.146	[25]
32	Cd(II)	Orange waste	17.3	0.230	180	28.5	0.152	[8]
33	Cr(II)	HT500	14.3	0.172	240	37.1	0.157	[6]
34	Tannic acid	Chitosan bead	150	0.012	270	516	0.161	[25]
35	<i>p</i> -Cresol	AC (FWKC1060)	618	0.0248	30	248	0.163	[20]
36	Pb(II)	FTAW	41.5	0.061	180	100	0.164	[5]
37	4-CP	AC (CobNa50)	1.27E3	0.0107	30	554	0.166	[21]
38	4-CP	AC (Cob4015)	935	0.0106	30	539	0.175	[26]
39	Humic acid	Chitosan bead	13.9	0.032	270	175	0.179	[25]
40	AO51	Chitosan bead	7.2	0.119	270	45.7	0.184	[25]
41	AB74	AC (FWKC1060)	235	0.0302	30	179	0.186	[20]
42	BR46	Clay-sawdust	31.0	0.232	30	23.2	0.186	[27]
43	MB	Chitosan bead	11.0	0.066	270	80.0	0.189	[25]
44	MB	AC (Cob4015)	412	0.0156	30	338	0.189	[26]
45	Pb(II)	Straw	21.2	0.050	180	104	0.192	[5]
46	MB	AC (FWKC1060)	409	0.0139	30	370	0.195	[20]
47	Phenol	AC (Cob4015)	179	0.0287	30	176	0.198	[26]
48	RR222	Chitosan bead	40.6	0.014	270	360	0.198	[25]
49	CV	Apricot AC	26.6	0.095	60	52.9	0.199	[23]
50	MB	AC (CPKC3)	338	0.0151	30	332	0.199	[22]
51	2,4-DCP	AC (Cob4015)	553	0.0088	30	564	0.201	[26]
52	Phosphate	Alunite	25.2	0.044	120	111	0.205	[28]
53	BB1	AC (CPKC3)	419	0.0085	30	549	0.214	[22]
54	AB74	AC (CPKC3)	96.1	0.0362	30	128	0.215	[22]
55	MB	AC (CobNa50)	332	0.0103	30	449	0.216	[21]
56	AB74	AC (Cob4015)	121	0.0276	30	167	0.217	[26]
57	4-NP	AC (FWKC1060)	137	0.0239	30	193	0.218	[20]
58	Cd(II)	Bone char	89.6	0.102	600	44.2	0.221	[29]
59	BB1	AC (Cob4015)	169	0.0155	30	282	0.229	[26]
60	Pb(II)	Clinoptilolite (P)	3.12	0.098	240	43.83	0.233	[30]
61	AB74	AC (CobNa50)	133	0.0179	30	238	0.245	[21]
62	Naphthalene	DAT zeolite	1.28	0.122	360	33.0	0.248	[31]
63	Pb(II)	Clinoptilolite (N)	1.52	0.100	240	35.96	0.278	[30]

When a specific x is considered (say, $x = 0.85$ at $t = t_{0.85}$), we obtain the following equation from Eq. (18):

$$\left(\frac{t_x}{t_{0.85}}\right) = \exp\left[\frac{(x - 0.85)}{R_E}\right] \quad (19)$$

Eq. (19) indicates the operating time t_x at an adsorbent capacity left x . In engineering, a decrease in both adsorbent capacity left and operating time can reduce the total cost. However, both factors

are actually in contradiction according to Eq. (19). The relationship between the two factors depends on the R_E value of adsorption system. A family of curves obtained from plotting $(t_x/t_{0.85})$ vs. R_E with x as a parameter are shown in Fig. 7. When x increases, adsorbent utilization increases (i.e., reducing adsorbent consumption); but $t_x/t_{0.85}$ also increases (i.e., increasing operation time). The evaluation of the optimal x value must be based on the engineering economics.

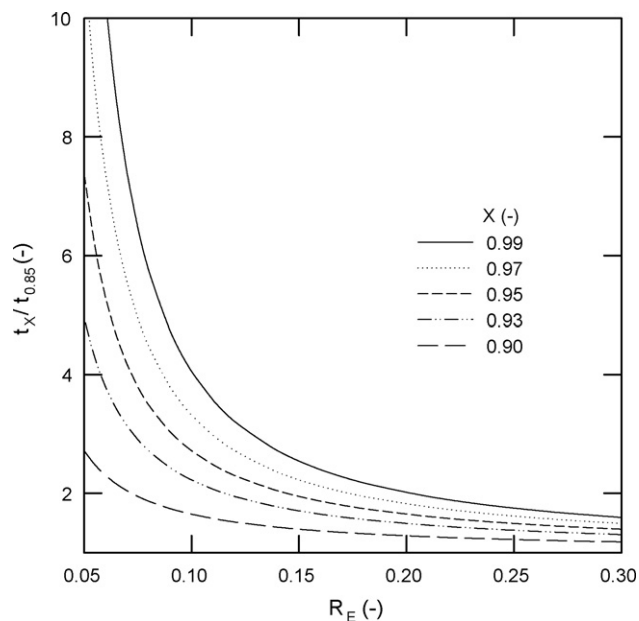


Fig. 7. Relationships between operating time ($t/t_{0.85}$) and approaching equilibrium parameter (R_E) based on Elovich equation at different q_t/q_{ref} values.

The evaluation of x value is outlined below. How long is $t_{0.85}$ of an adsorption system? If $t_{0.85}$ is small, the x value can be high. For example, the R_E value of the adsorption of RR222 on DP3 is 0.167 in this study, and the $t_{0.85}$ value is 187 min (Eq. (7)). When the saving in adsorbent consumption is 5, 10, and 14%, then the increase in operating time is 65, 153, and 245 min, respectively. This means that an increase of operation time by 88 min is needed for a saving of adsorbent from 5 to 10%. On the other hand, an increase of 92 min is needed when a saving of adsorbent increases from 10 to 14%. Generally speaking, a high x value is preferred if the adsorbent cost is high. Of course, the content of adsorption system and the regeneration time of adsorbent should be also considered when x value is to be selected.

5. Conclusions

The characteristic adsorption curves involving Elovich equation has been deduced. The dimensionless group ($1/q_{ref}b$) was defined as the approaching equilibrium parameter (R_E). Four zones were classified based on R_E value. Of 64 adsorption systems searched from literature, 80% belong to the zone of "mild adsorption" and 20% to the zone of "rapid adsorption". The characteristic curve based on Elovich equation was between those of Lagergren's first-order equation and intraparticle diffusion model.

The chitosans derived from three raw materials were used for kinetic studies on adsorption of reactive dye RR222. The results of standard deviation (S.D.) indicated that the Elovich equation was superior to the Lagergren's first-order equation and intraparticle diffusion model for the description of adsorption kinetics. The adsorption behavior was classified to zone II, the region of "mild adsorption". The R_E values obtained in the adsorption on chitosans with three different particle sizes were almost the same, reflecting the nature of chemical adsorption of Elovich equation. The relationship between x value and the operating time ($t_x/t_{0.85}$) could be thus built according to an 85% of adsorbent consumption ($x=0.85$) and corresponding operating time ($t_{0.85}$). This allowed us to easily select an optimal x value for engineering practice.

Acknowledgment

Financial support of this work by the National Science Council, R.O.C., under contract No. NSC96-2221-E-239-021 is gratefully acknowledged.

References

- C. Aharoni, F.C. Tompkins, Kinetics of adsorption and desorption and the Elovich equation, in: D.D. Eley, H. Pines, P.B. Weisz (Eds.), *Advances in Catalysis and Related Subjects*, vol. 21, Academic Press, New York, 1970, pp. 1–49.
- R.S. Juang, M.L. Chen, Application of the Elovich equation to the kinetics of metal sorption with solvent-impregnated resins, *Ind. Eng. Chem. Res.* 36 (1997) 813–820.
- F.C. Wu, R.L. Tseng, R.S. Juang, Adsorption of dyes and humic acid from water using chitosan encapsulated activated carbon, *J. Chem. Technol. Biotechnol.* 77 (2002) 1269–1279.
- R.L. Tseng, F.C. Wu, R.S. Juang, Liquid-phase adsorption of dyes and phenols using pinewood-based activated carbons, *Carbon* 41 (2003) 487–495.
- A. Örnek, M. Özacar, I.A. Sengil, Adsorption of lead onto formaldehyde or sulfuric acid treated acorn waste: equilibrium and kinetic studies, *Biochem. Eng. J.* 37 (2007) 192–200.
- N.K. Lazaridis, D.D. Asouhidou, Kinetics of sorptive removal of chromium(VI) from aqueous solution by calcined Mg–Al–CO₃ hydroxalcite, *Water Res.* 37 (2003) 2875–2882.
- R.R. Sheha, A.A. El-Zahhar, Synthesis of some ferromagnetic composite resins and their metal removal characteristics in aqueous solutions, *J. Hazard. Mater.* 150 (2008) 795–803.
- A.B. Pérez-Marín, V.M. Zapata, J.F. Ortuño, M. Aguilar, J. Sáez, M. Llorens, Removal of cadmium from aqueous solutions by adsorption onto orange waste, *J. Hazard. Mater.* 139 (2007) 122–131.
- E. Malkoc, Y. Nuhoglu, Determination of kinetic and equilibrium parameters of batch adsorption of Cr(VI) onto waste acorn of *Quercus ithaburensis*, *Chem. Eng. Process.* 46 (2007) 1020–1029.
- T.S. Anirudhan, P.G. Radhakrishnan, Chromium(III) removal from water and wastewater using a carboxylate-functionalized cation exchanger prepared from a lignocellulosic residue, *J. Colloid Interface Sci.* 316 (2007) 268–276.
- R. Han, W. Zou, Z. Zhang, J. Shi, J. Yang, Removal of copper(II) and lead(II) from aqueous solution by manganese oxide coated sand. I. Characterization and kinetic study, *J. Hazard. Mater.* 137 (2006) 384–395.
- K.H. Goh, T.T. Lim, Geochemistry of inorganic arsenic and selenium in a tropical soil: effect of reaction time, pH, and competitive anions on arsenic and selenium adsorption, *Chemosphere* 55 (2004) 849–859.
- X. Guo, L. Zeng, X. Li, H.S. Park, Ammonium and potassium removal for anaerobically digested wastewater using natural clinoptilolite followed by membrane pretreatment, *J. Hazard. Mater.* 151 (2008) 125–133.
- R.S. Juang, R.L. Tseng, F.C. Wu, S.H. Lee, Adsorption behavior of reactive dyes from aqueous solutions on chitosan, *J. Chem. Technol. Biotechnol.* 70 (1997) 391–399.
- R.S. Juang, R.L. Tseng, F.C. Wu, S.J. Lin, Use of chitin and chitosan in lobster shell wastes for color removal from aqueous solutions, *J. Environ. Sci. Health A* 31 (1996) 325–338.
- M.Y. Chang, R.L. Tseng, F.C. Wu, Relationship between the preparation conditions of chitosan and its adsorption ability, *J. Chin. Agric. Chem. Soc.* 36 (1998) 293–299.
- E. Guibal, I. Saucedo, M. Jansson-Charrier, B. Delanghe, P. Le Cloirec, Uranium and vanadium sorption by chitosan and derivatives, *Water Sci. Technol.* 30 (1994) 183–190.
- A. Kuleyin, Removal of phenol and 4-chlorophenol by surfactant-modified natural zeolite, *J. Hazard. Mater.* 144 (2007) 307–315.
- L. Zeng, X. Li, J. Liu, Adsorptive removal of phosphate from aqueous solutions using iron oxide tailings, *Water Res.* 38 (2004) 1318–1326.
- F.C. Wu, R.L. Tseng, Preparation of highly porous carbon from fir wood by KOH etching and CO₂ gasification for adsorption of dyes and phenols from water, *J. Colloid Interface Sci.* 294 (2006) 21–30.
- R.L. Tseng, Mesopore control of high surface area NaOH-activated carbon, *J. Colloid Interface Sci.* 303 (2006) 494–502.
- R.L. Tseng, S.K. Tseng, Characterization and use of high surface area activated carbons prepared from cane pith for liquid-phase adsorption, *J. Hazard. Mater.* 136 (2006) 671–680.
- Y. Önal, Kinetics of adsorption of dyes from aqueous solution using activated carbon prepared from waste apricot, *J. Hazard. Mater.* 137 (2006) 1719–1728.
- C. Namasivayam, K. Prathap, Adsorptive removal of silica onto 'waste' Fe(III)/Cr(III) hydroxide: kinetics and isotherms, *Colloids Surf. A: Physicochem. Eng. Aspects* 295 (2007) 55–60.
- M.Y. Chang, R.S. Juang, Equilibrium and kinetic studies on the adsorption of surfactant, organic acids and dyes from water onto natural biopolymers, *Colloids Surf. A: Physicochem. Eng. Aspects* 269 (2005) 35–46.
- R.L. Tseng, S.K. Tseng, F.C. Wu, Preparation of high surface area carbons from corn cob with KOH etching plus CO₂ gasification for the adsorption of dyes and phenols from water, *Colloids Surf. A: Physicochem. Eng. Aspects* 279 (2006) 69–78.
- N. Yeddou, A. Bensmaili, Kinetic models for the sorption of dye from aqueous solution by clay-wood sawdust mixture, *Desalination* 185 (2005) 499–508.

- [28] M. Özacar, Contact time optimization of two-stage batch adsorber design using second-order kinetic model for the adsorption of phosphate onto alunite, *J. Hazard. Mater.* 137 (2006) 218–225.
- [29] E.F. Covelo, M.L. Andrade, F.A. Vega, Heavy metal adsorption by humic umbrilsols: selectivity sequences and competitive sorption kinetics, *J. Colloid Interface Sci.* 280 (2004) 1–8.
- [30] A. Günay, E. Arslankaya, I. Tosun, Lead removal from aqueous solution by natural and pretreated clinoptilolite: adsorption equilibrium and kinetics, *J. Hazard. Mater.* 146 (2007) 362–371.
- [31] C.F. Chang, C.Y. Chang, K.H. Chen, W.T. Tsai, J.L. Shie, Y.H. Chen, Adsorption of naphthalene on zeolite from aqueous solution, *J. Colloid Interface Sci.* 277 (2004) 29–34.